Scientific Research Publishing

International Journal of Geosciences, 2024, 15, 40-53
https://www.scirp.org/journal/ijg
ISSN Online: 2156-8367
ISSN Print: 2156-8359

The Impact of Model Based Offset Scaling Technique on the Amplitude Variation with Offset Responses from 3D Seismic Data Acquired from the Tano Basin, Offshore Ghana

Striggner Bedu-Addo*, Sylvester Kojo Danuor, Aboagye Menyeh

Department of Physics, Kwame Nkrumah University of Science and Technology, Kumasi, Ghana
Email: *striggnerbeduaddo@gmail.com

How to cite this paper: Bedu-Addo, S., Danuor, S.K. and Menyeh, A. (2024) The Impact of Model Based Offset Scaling Technique on the Amplitude Variation with Offset Responses from 3D Seismic Data Acquired from the Tano Basin, Offshore Ghana. *International Journal of Geosciences*, **15**, 40-53.
https://doi.org/10.4236/ijg.2024.151004

Received: December 28, 2023
Accepted: January 28, 2024
Published: January 31, 2024

Abstract

Amplitudes have been found to be a function of incident angle and offset. Hence data required to test for amplitude variation with angle or offset needs to have its amplitudes for all offsets preserved and not stacked. Amplitude Variation with Offset (AVO)/Amplitude Variation with Angle (AVA) is necessary to account for information in the offset/angle parameter (mode converted S-wave and P-wave velocities). Since amplitudes are a function of the converted S- and P-waves, it is important to investigate the dependence of amplitudes on the elastic (P- and S-waves) parameters from the seismic data. By modelling these effects for different reservoir fluids via fluid substitution, various AVO geobody classes present along the well and in the entire seismic cube can be observed. AVO analysis was performed on one test well (Well_1) and 3D pre-stack angle gathers from the Tano Basin. The analysis involves creating a synthetic model to infer the effect of offset scaling techniques on amplitude responses in the Tano basin as compared to the effect of unscaled seismic data. The spectral balance process was performed to match the amplitude spectra of all angle stacks to that of the mid (26˚) stack on the test lines. The process had an effect primarily on the far (34˚ - 40˚) stacks. The frequency content of these stacks slightly increased to match that of the near and mid stacks. In offset scaling process, the root mean square (RMS) amplitude comparison between the synthetic and seismic suggests that the amplitude of the far traces should be reduced relative to the nears by up to 16%. However, the exact scaler values depend on the time window considered. This suggests that the amplitude scaling with offset delivered from seismic processing is only approximately correct and needs to be checked

with well synthetics and adjusted accordingly prior to use for AVO studies. The AVO attribute volumes generated were better at resolving anomalies on spectrally balanced and offset scaled data than data delivered from conventional processing. A typical class II AVO anomaly is seen along the test well from the cross-plot analysis and AVO attribute cube which indicates an oil filled reservoir.

Keywords

Amplitude Variation with Offset (AVO), Model Based Offset Scaling Technique, Tano Basin

1. Introduction

The motivation for hydrocarbon exploration using passive or active geophysical methods is to detect/discover potential oil and natural gas deposits embedded in subsurface geological structures. A prospective subsurface geological structure must be identified with an impermeable seal, a migration path, reservoir rock, and a mature source rock [1]. For hydrocarbons to build and be preserved, the relative timing of these elements' synthesis as well as the processes of generation, migration, and accumulation must be correct [2]. One of such geophysical techniques is seismic survey, which differs in how it is used onshore (land) and offshore (marine). The fundamental ideas are the same: initiate a seismic pulse at or near the earth's surface using a seismic source and record the amplitudes and travel times of waves that are reflected or refracted from the boundaries between two layers. To generate bursts of sound energy, a ship usually tows a submerged energy source, such as an air or water gun, when conducting seismic surveys in offshore locations. The difference in water pressure with respect to hydrostatic pressure is then measured using a long streamer equipped with several hydrophones. But in land survey, a cable runs from the shot site using dynamite or a vibrator in one or both directions connect geophones or receiver groups that measure the particle velocity of the ground to a recording truck. When acquiring data for land and marine surveys, seismic sources and receivers are used to sample every point in the subsurface several times. This results in a unique angular relationship between the source, sample location (reflection point), and receiver for each sample (trace) [3]. The magnitude of the amplitudes of these traces increases, decreases or remains constant with changing angles of incidence or offset (distance between the shot and receiver) with respect to the reflection coefficient (contrast in density, compressional velocity and shear velocity across the boundary) as defined in Equations (1.1) and (1.2) using Zeoppritz equation and Shuey's two-term approximation respectively.

$$R = \frac{a_{\text{reflected}}}{a_{\text{incident}}} = \frac{Z_2 - Z_1}{Z_2 + Z_1} = \frac{\rho_2 v_2 - \rho_1 v_1}{\rho_2 v_2 + \rho_1 v_1} \tag{1.1}$$

where $\rho_1, v_1, Z_1, \rho_2, v_2$ and Z_2 are the densities, velocities, and impedances of the first and second layer, and R or $R(0)$ is the P-wave reflection coefficient at normal incidence, which forms the basis for AVO effects.

$$R(\theta) = A + B\sin^2\theta + \cdots \tag{1.2}$$

Shuey's two-term approximation, which is defined in Equation (1.2), can be used to illustrate the angular dependency of the P-wave reflection coefficient $R(\theta)$ that was previously mentioned. Where B represents the variation at intermediate offsets, known as the AVO gradient, and A is the normal-incident reflection coefficient (intercept). Although the far offset near critical angle is dominated by the third term of Equation (1.2), less than 30˚ - 40˚ angles are accessible for AVO research. Thus, for angles less than 30˚, it is necessary to consider only the first two terms [4]. As pointed out by [5] and [6], the extraction of these two parameters from seismic, when cross-plotted, normally generates a distinct background trend in the absence of hydrocarbon-bearing strata; any variation from this background trend can be interpreted as a hydrocarbon indicator. However, some of the pitfalls of AVO are attributed to the use of non-representative amplitudes in AVO modelling. This is because of the use of scaling functions and normal move out procedures used during seismic processing to correct transmissivity effects such as Differential interference (tuning), Mode Conversions (P-S-P), Attenuation (Q), Critical angle effects and Anisotropy. These procedures introduce low frequencies at the far offset and distort the traces. This suggest that there is the need to balance the spectra and scale the amplitudes to ensure amplitude and frequency fidelity. The practice in most scenarios is that these distortions are muted surgically and predicted statistically by averaging the Nears and Mids traces using scaling function algorithms which introduce too many uncertainties in the far offset amplitudes for AVO predictions. To avoid drilling dry wells as has been observed in the offshore basin, Ghana, due to over estimation of seismic amplitudes resulting in out-of-phase AVO artifacts. There is the need to recalibrate the amplitude scaling with offset delivered from seismic processing with well synthetics to ensure representative amplitudes and corrected frequencies in seismic gathers used for AVO modelling. This paper seeks to investigate the impact of model based offset scaling technique on amplitude variation with offset responses from 3D seismic data acquired from the Tano basin, offshore Ghana, to resolve low frequencies and distortions introduced at the far offsets from normal move-out procedures and scaling functions used during seismic processing by balancing the spectra and scaling the amplitudes to ensure amplitude and frequency fidelity for AVO modelling.

2. Study Area

The Tano Basin is situated in the Gulf of Guinea in Ghana's southern-eastern region. With the exception of a small amount of land extension, the majority of

the Tano Basin is offshore and lies between latitudes 4˚48'N and longitude 2˚47'W, East; 4˚47'N and longitude 2˚52'W, West; 4˚49'N and longitude 2˚47'W, North; and 4˚46'N and longitude 2˚52'W, South. The area of the basin, which has shown to have significant hydrocarbon potential, is situated 60 km offshore Ghana and has a sea depth of between 1200 and 1500 km [7] [8].

3. Materials and Method

3.1. Dataset

To investigate the impact of model-based scaling technique on amplitude variation with offset responses from 3D seismic data acquired from the Tano Basin, offshore Ghana, the under listed materials were used to generate the AVO anomalies in the Tano Basin.

- 3D Seg-y Pre-stack Angle Gathers, CDP Gathers from Tano Basin.
- Velocity cube.
- One Explorational Well (Well_1).
- Hampson-Russell Software.

3.2. Methodology

To investigate the impact of model base offset scaling technique on AVO responses in the Tano Basin, AVO responses from unscaled and scaled data were compared. This was done in two phases, Case I and Case II. In case I, AVO studies were conducted on seismic gathers delivered from traditional processing methods (unscaled seismic gathers). Whereas in case II, AVO studies were conducted on module-based offset scaled seismic gathers. The results from both cases were compared to ascertain the approach that better imaged the AVO anomaly. In both cases, the workflow for loading all the input data into Geoview of Hampson-Russell included the following:

1) Load Well Data.
2) Load Seismic Data.
3) Pick Horizons.
4) Load Velocity cube.

After loading all the input data, cursory editing of the well logs was done to remove spikes attributable to instrument errors and borehole conditions, and the three vintages of seismic data was checked for quality. **Figure 1** shows the final near stack cube generated as was done for the mid and far stack cubes.

3.2.1. Wavelet Extraction

The statistical wavelet was extracted first to allow for minimum degree of correlation between the well and the seismic data. To ensure a more representative wavelet, a wavelet was also extracted using the well within the reservoir or zone of interest as shown in **Figure 2** and **Figure 3**.

3.2.2. Well Correlation

The well was correlated to the seismic to.

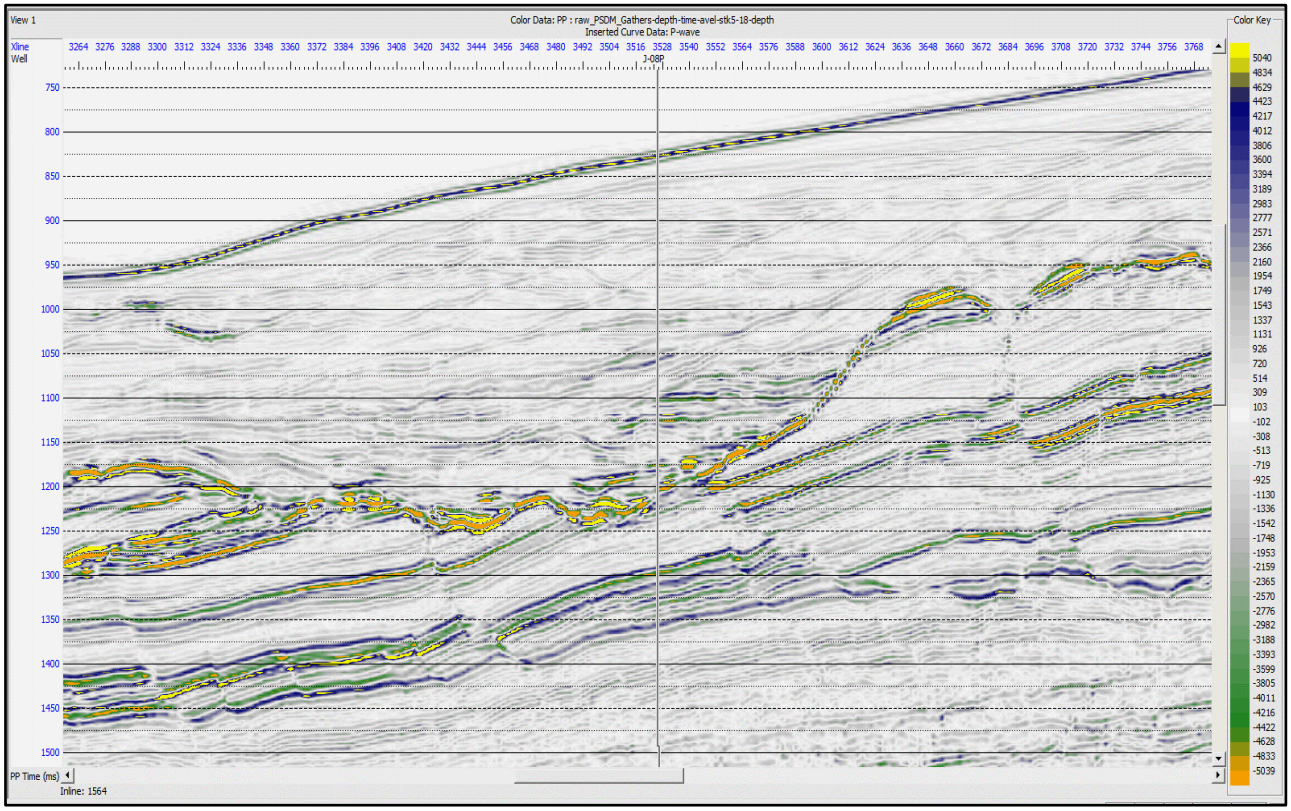

Figure 1. Final loaded near stack cube (5˚ - 18˚).

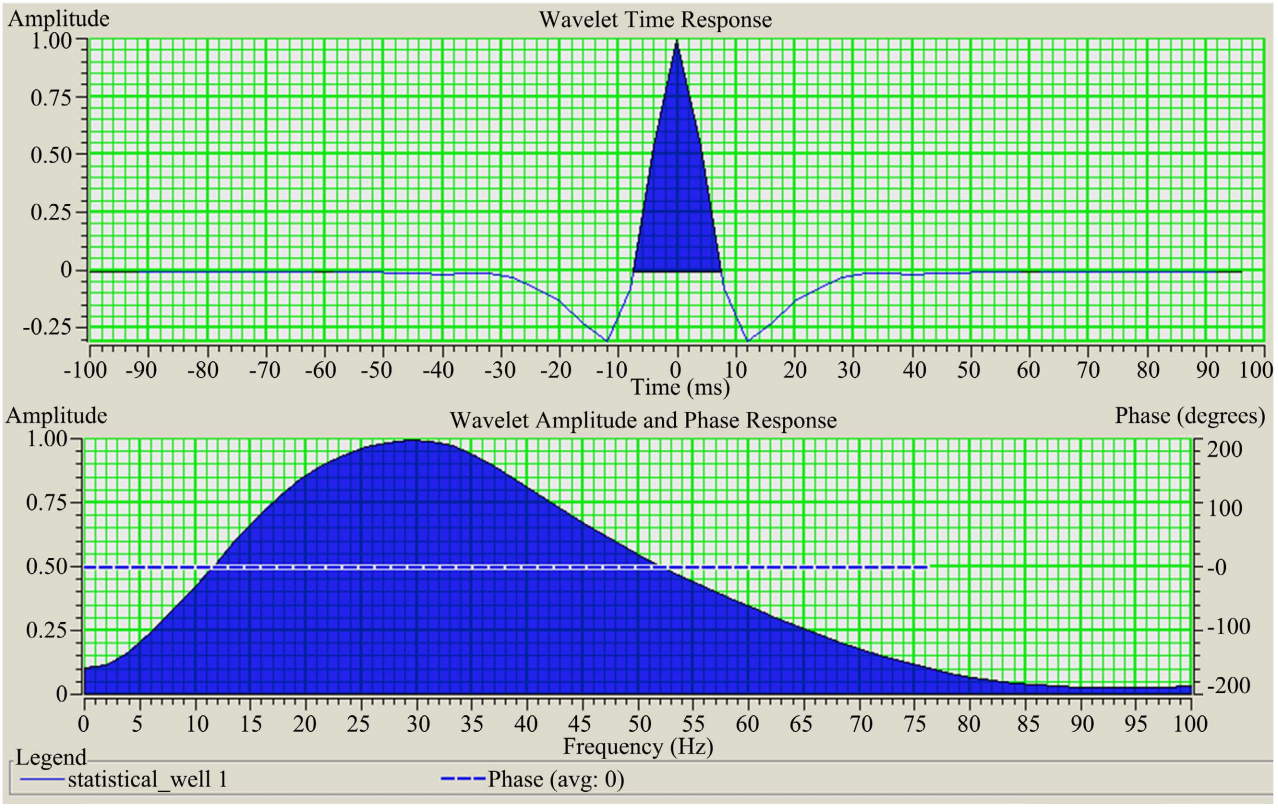

Figure 2. Extracted statistical wavelet: (a) Wavelet time response, (b) Wavelet amplitude and phase response.

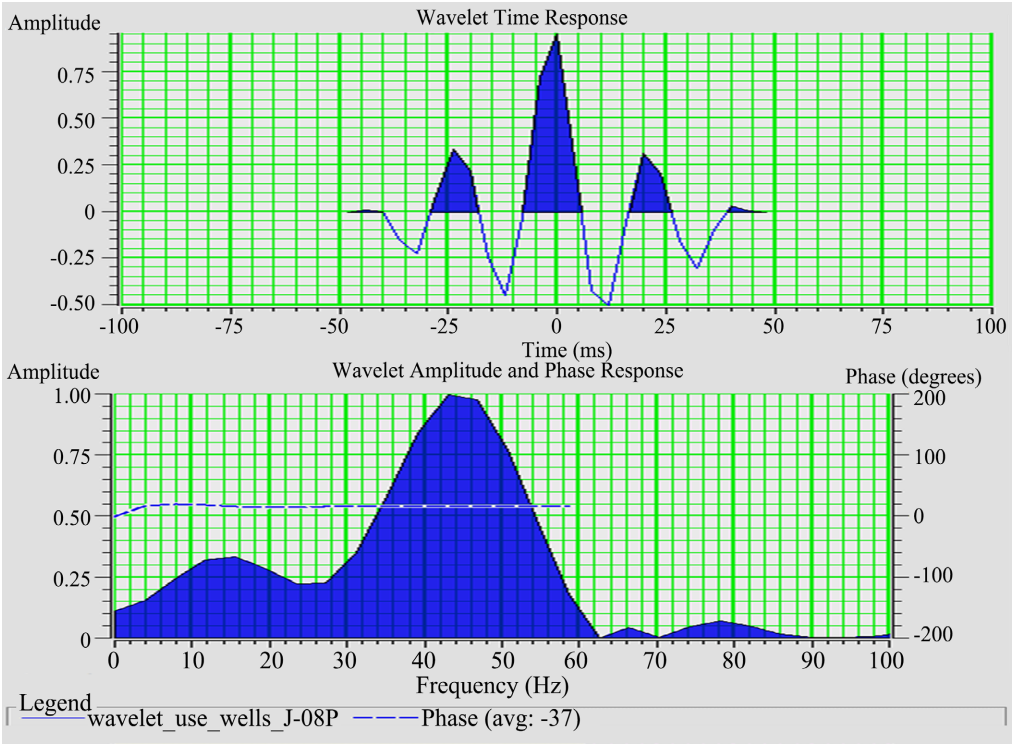

Figure 3. Wavelet extraction using wells: (a) Wavelet time response, (b) Wavelet amplitude and phase response.

1) Ultimately tie the well to the seismic to ensure that the well and seismic are accurately correlatable.

2) Correct the check shots.

3) Upscale the well logs to seismic frequencies through the convolution process of wavelet and reflectivity (**Figure 4**).

3.2.3. AVO Gradient Analysis

AVO gradient analysis was done to check for trace alignment in the gathers. This was to ensure that events are well aligned to conduct the AVO process successfully and to check the AVO response along the well locations.

3.2.4. AVO Attribute Volumes

AVO Intercept, Gradient, product of intercept and gradient and the scaled Poisson Ratio change attribute volumes were generated using the workflow in **Figure 5** to enhance AVO analysis within the seismic cube (**Figure 12**).

3.2.5. Model-Based Scaling

In model-based scaling, forward modelling was used to simulate synthetic seismic traces for a given subsurface model. The synthetic traces were then compared with the observed seismic data, and scaling factors are adjusted to minimize the misfit. To match the observed and the synthetic responses, apply the scaling factors obtained from the modelling process to the seismic data as shown in **Figure 6**.

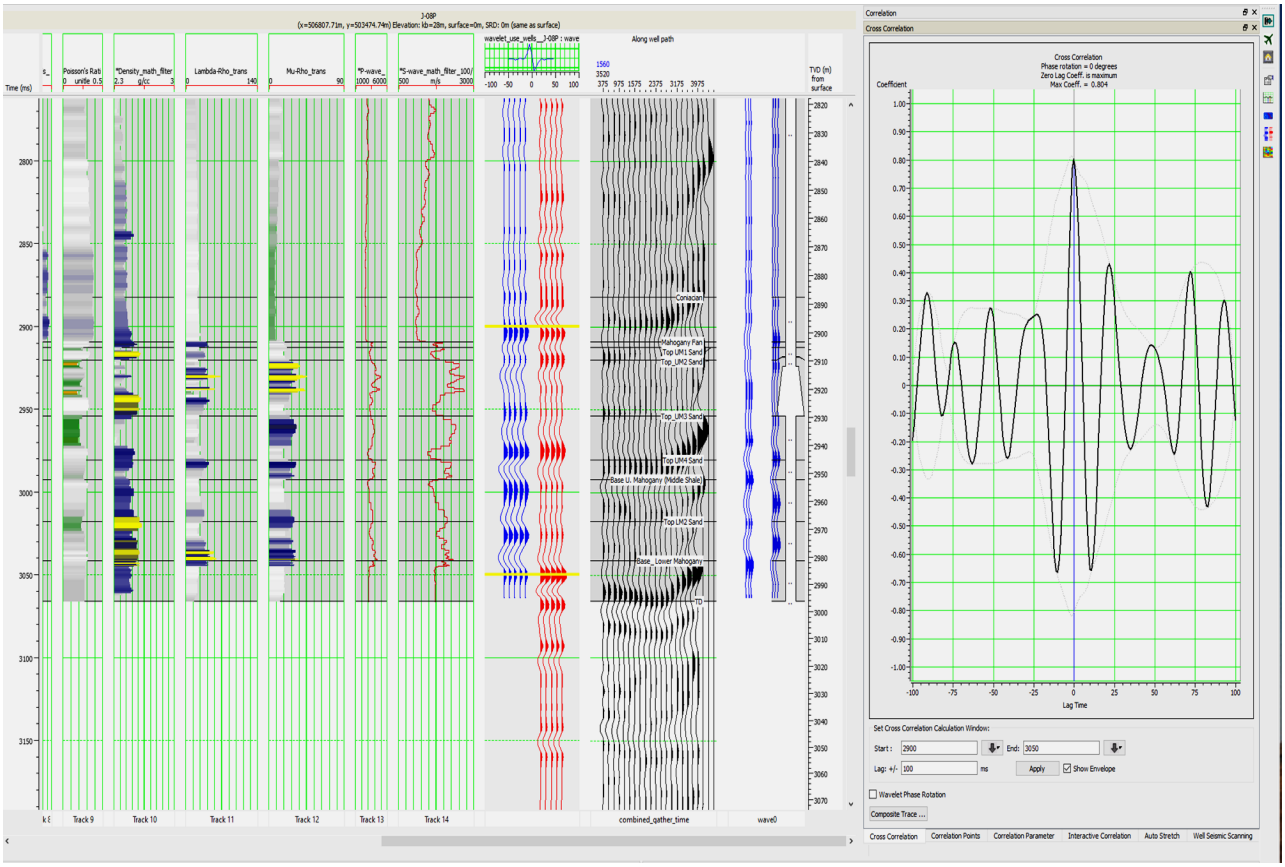

Figure 4. Correlation window showing a correlation coefficient of 0.8.

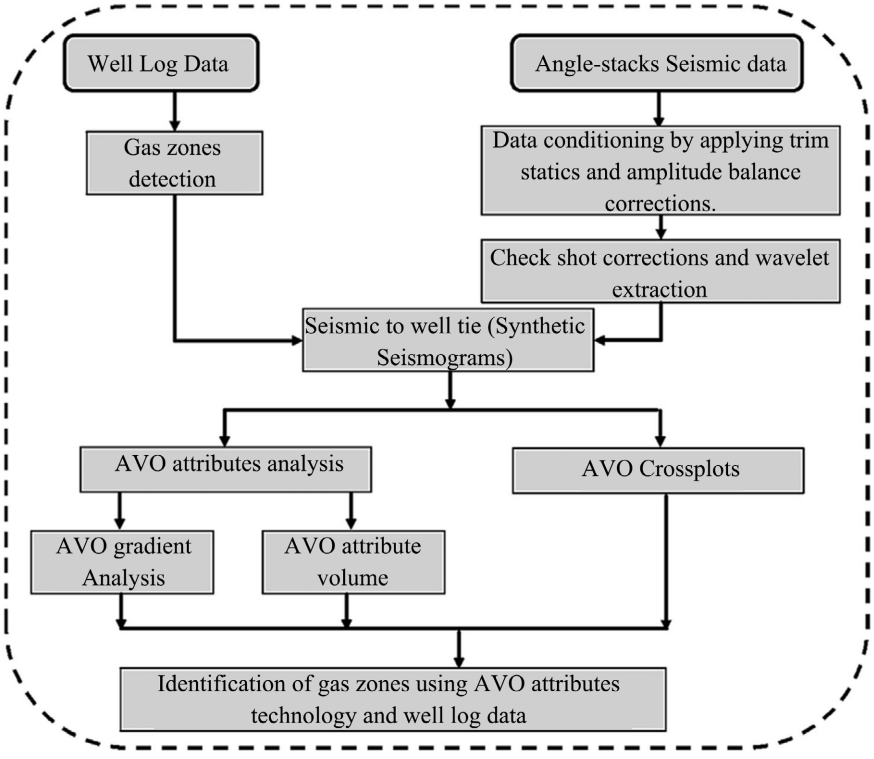

Figure 5. Workflow for AVO modeling.

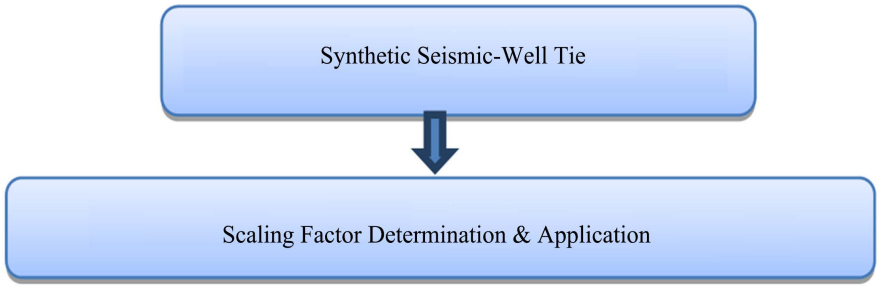

Figure 6. Workflow for model-based scaling.

1) Synthetic seismic well tie

1) Compare the synthetic seismic traces generated with the observed seismic data at the well location.

2) Adjust the scaling factors in the modelling of the rock physics iteratively to minimize the misfit between the synthetic and observed seismic traces.

3) Utilize techniques such as least squares fitting or cross-correlation to optimize the scaling factors to achieve a satisfactory match between the synthetic and observed seismic responses.

2) Scaling factor application

1) Apply the optimized scaling factors obtained from the synthetic seismic-well tie to the angle stack seismic data.

2) Scale the seismic amplitudes for each offset angle or offset bin to account for the amplitude variation with offset based on the scaling factors determined from the well tie.

3) Ensure that the scaling is consistently applied across all traces in the angle stack seismic data, maintaining the relative amplitudes between different offsets (Table 1).

The trend of scalers realized from the scaler modelling was seen to be indicative of amplitude distortions in the far angle gathers compared to the near angle gathers. This further emphasizes the need to deploy a geologically fit amplitude scaling technique such as the model-based technique used in this scenario. From Figure 7 the far angle gathers at 51˚ had amplitude attenuations of close to 16% whiles the mid angle gathers at 27˚ and 39˚ have amplitude attenuations of about 6%. The very near angle gathers (5˚ - 15˚) have relatively no amplitude attenuations. In other to correct for these amplitude distortions the scalers generated are applied to the seismic gathers to restore the attenuated amplitudes prior to AVO work.

3.2.6. Percentage Error (%E) Determination

The degree of Amplitude distortion was quantified in the Model-Based Offset Scaling by (3.1) to determine the degree of attenuation at the far angle to be corrected.

$$\text{Percentage Error}(\%E) = \frac{\text{Seismic} - \text{Synthetic}}{\text{Seismic}} \times 100\% \quad (3.1)$$

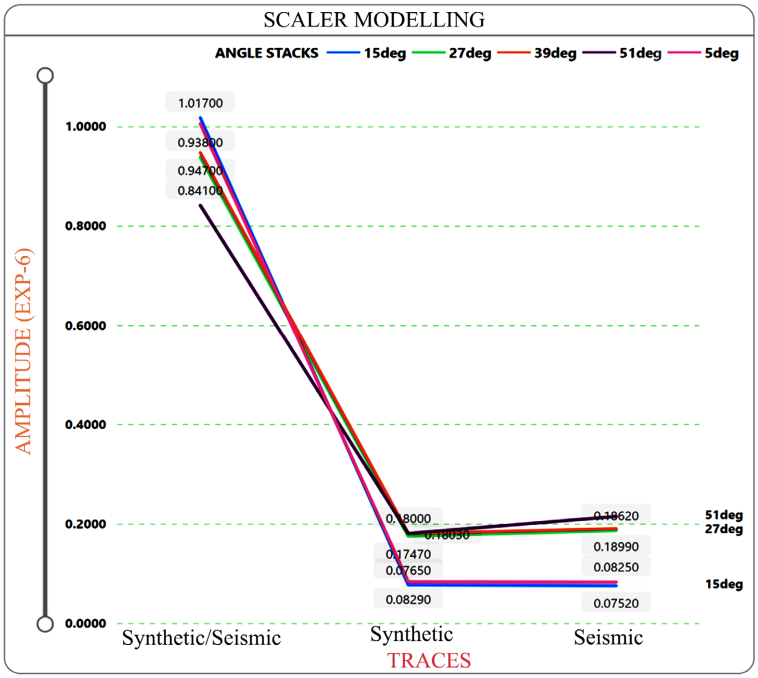

Figure 7. Scalers generated for individual angle stacks for synthetic and seismic traces.

Table 1. Shows the scalars generated for the individual angle stacks.

AmpxE-6	5 deg	15 deg	27 deg	39 deg	51 deg
Synthetic	0.0829	0.0765	0.1747	0.1800	0.1803
Seismic	0.0825	0.0752	0.1862	0.1899	0.2145
Synth/Seismic	1.005	1.017	0.938	0.947	0.841

4. Results

Case I.

4.1. AVO Attribute Volumes without Offset Scaling

AVO attributes were generated for the entire data volume. The Scaled Poisson Ratio change volume indicates Poisson ratio changes in and out of the reservoir. Reservoir measurements of Poisson ratio are generally lower compared to out of reservoir measurements. Therefore, a decrease or negative change is expected as you enter the reservoir from the overlying formation and a corresponding increase or positive change is observed as you exit the reservoir to the underlying formation. This is seen in the colour key representation. Hence potential reservoirs are easily mapped using this attribute as seen in the **Figure 8**.

From **Figure 9** the AVO attribute of product and gradient can identify class III and II AVO anomalies as these have a negative intercept and a negative gradient. The product of two negatives is a positive. The other AVO classes will produce negative product of gradient and intercept. Therefore, Class III/II AVO anomalies are seen as positive (red) values in this attribute volume. The top and base of the reservoir will both have the same colour, *i.e.*, red.

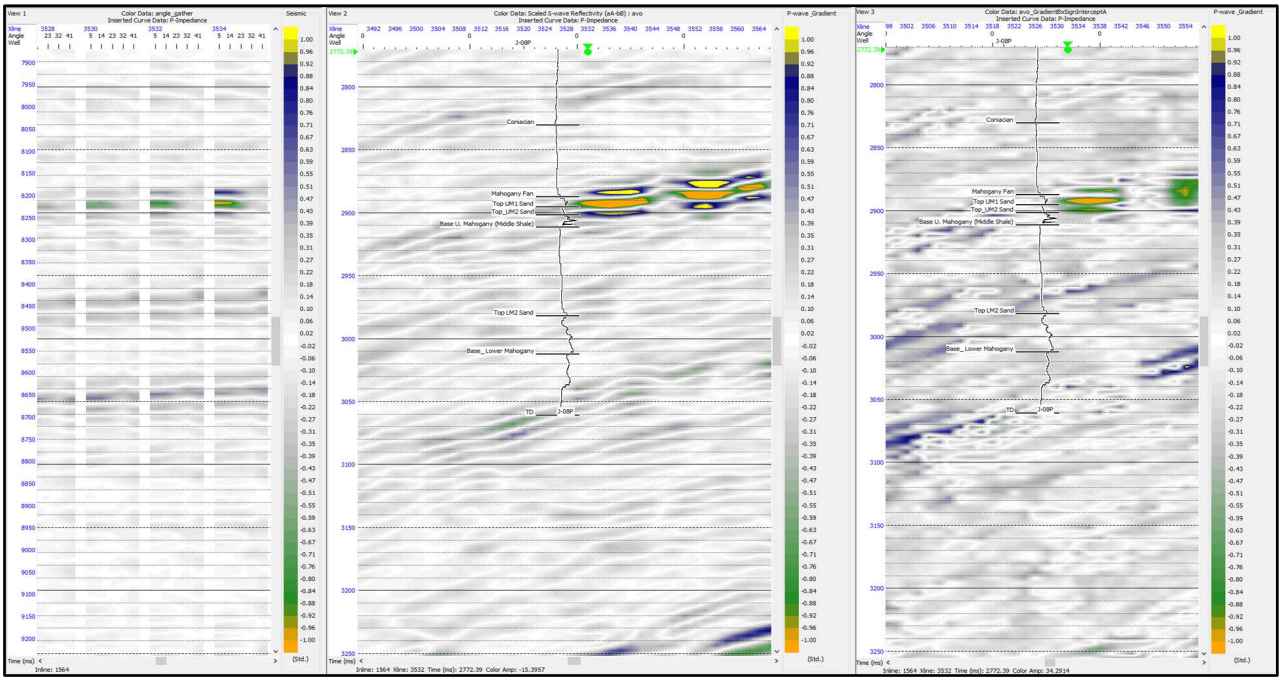

Figure 8. (b) AVO attribute volume of scaled Poisson ratio change along the test well. (c) Gradient * Sign Intercept A.

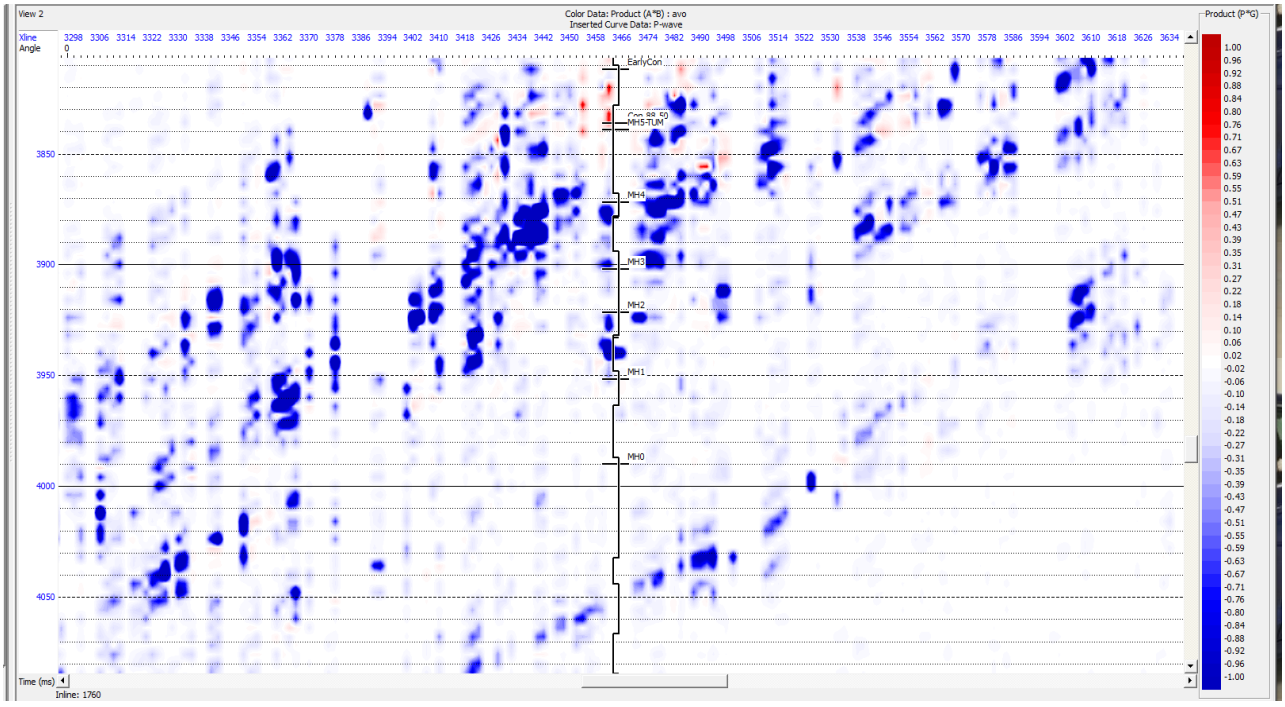

Figure 9. Showing AVO attribute of product of intercept and Gradient along the well.

Case II.

4.2. Spectral Balancing & Offset Scaling

From **Figure 10**, larger amplitude variations are observed in the higher frequency range of the amplitude spectra. For reasons such as inelastic attenuation,

diffraction, spherical divergence, normal moveout (NMO) stretch and migration effects there is a loss of high frequency and an increase in low frequencies with offset or angle. This suggest that there is a need to balance the spectra to ensure amplitude and frequency fidelity (Figure 11).

4.3. AVO Attribute Volumes after Spectral Balancing & Offset Scaling

The reservoir sand facies have been clearly imaged in Figure 12 after Spectral Balancing compared to the same attribute generated for the Amplitude Gain Control (AGC) applied data or the unscaled data. Lateral continuity of reservoir facies is more pronounced after Spectral Balancing than AGC. At the top of the reservoir, Poisson Ratio is expected to decrease (in this case negative) shown by the orange colour and increase at the base of the reservoir (in this case positive)

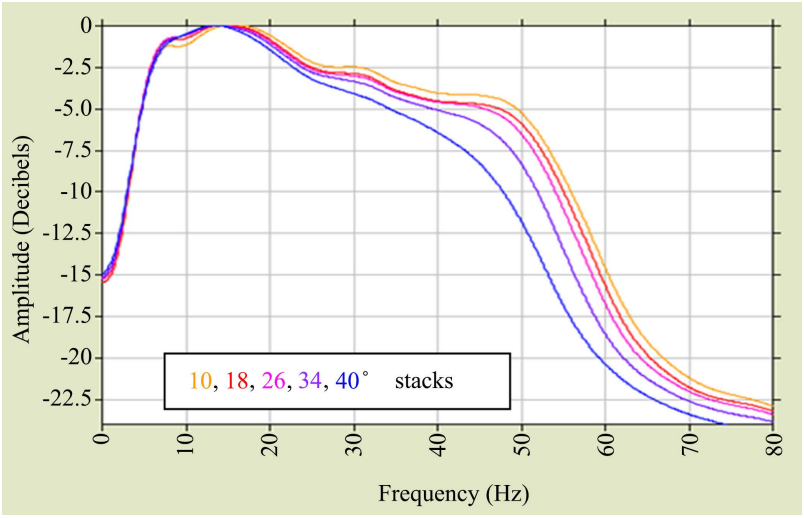

Figure 10. Amplitude spectra before spectral balancing.

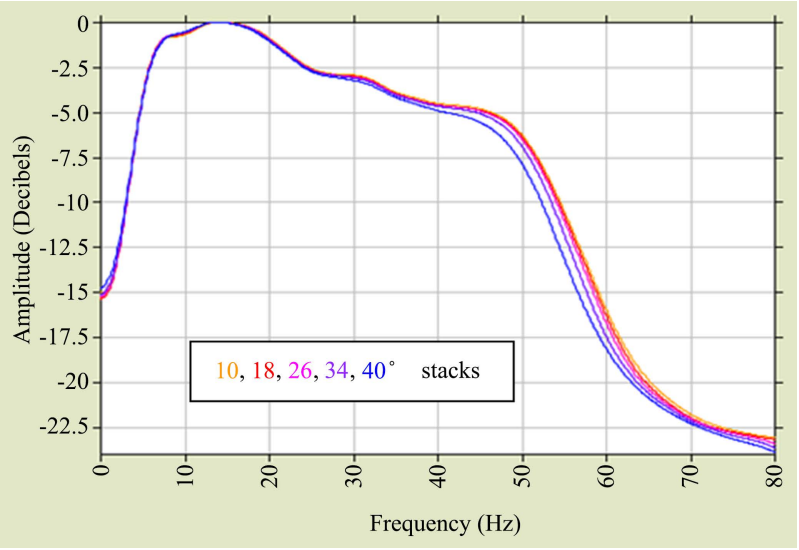

Figure 11. Amplitude spectra after spectral balancing.

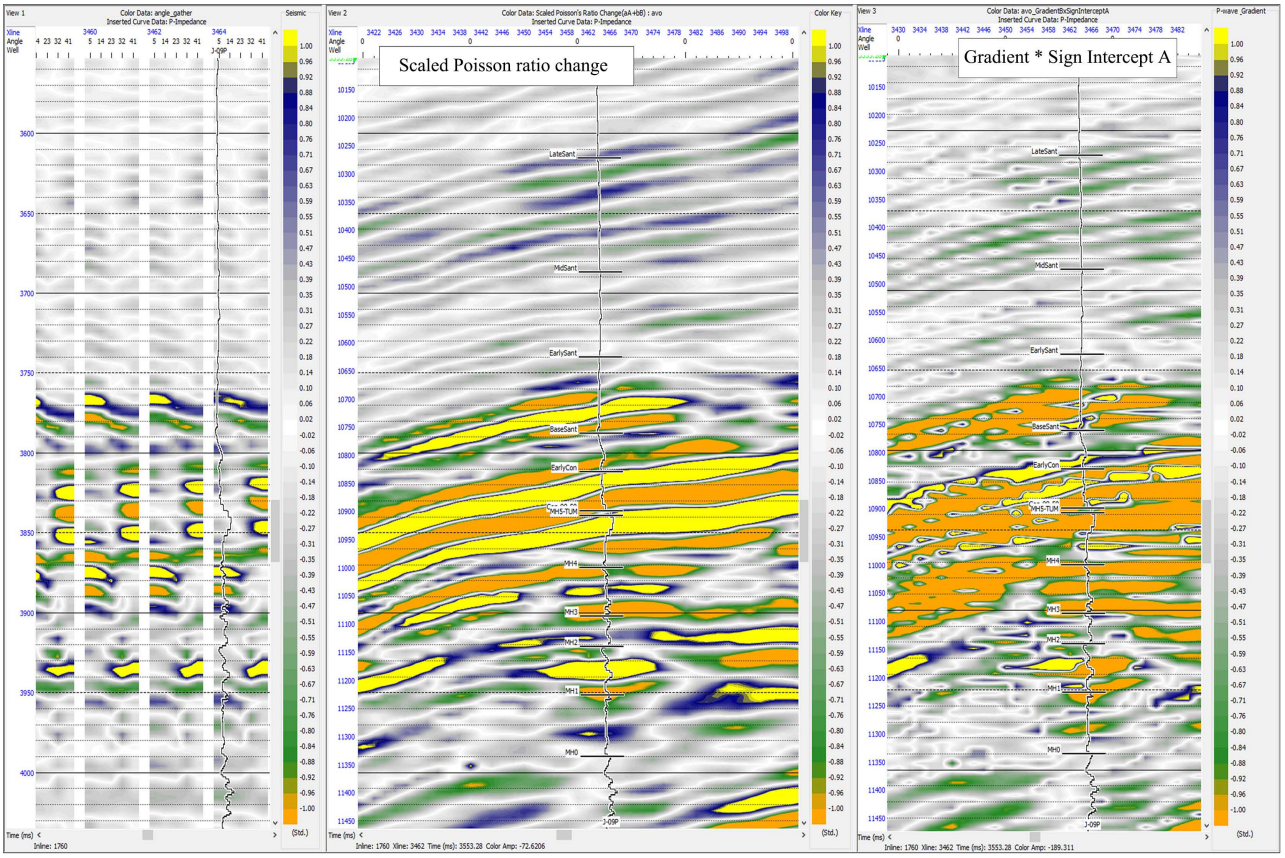

Figure 12. (b) Showing the scaled poisson ratio change after spectral balancing and offset scaling. (c). AVO Gradient * Sign Intercept attribute.

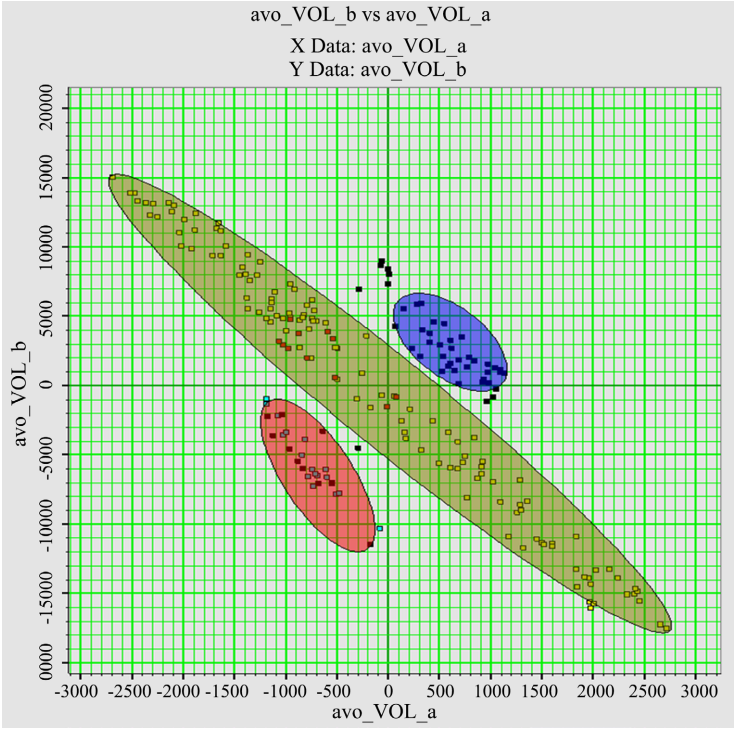

Figure 13. Intercept-gradient Crossplot of gradient and intercept volumes.

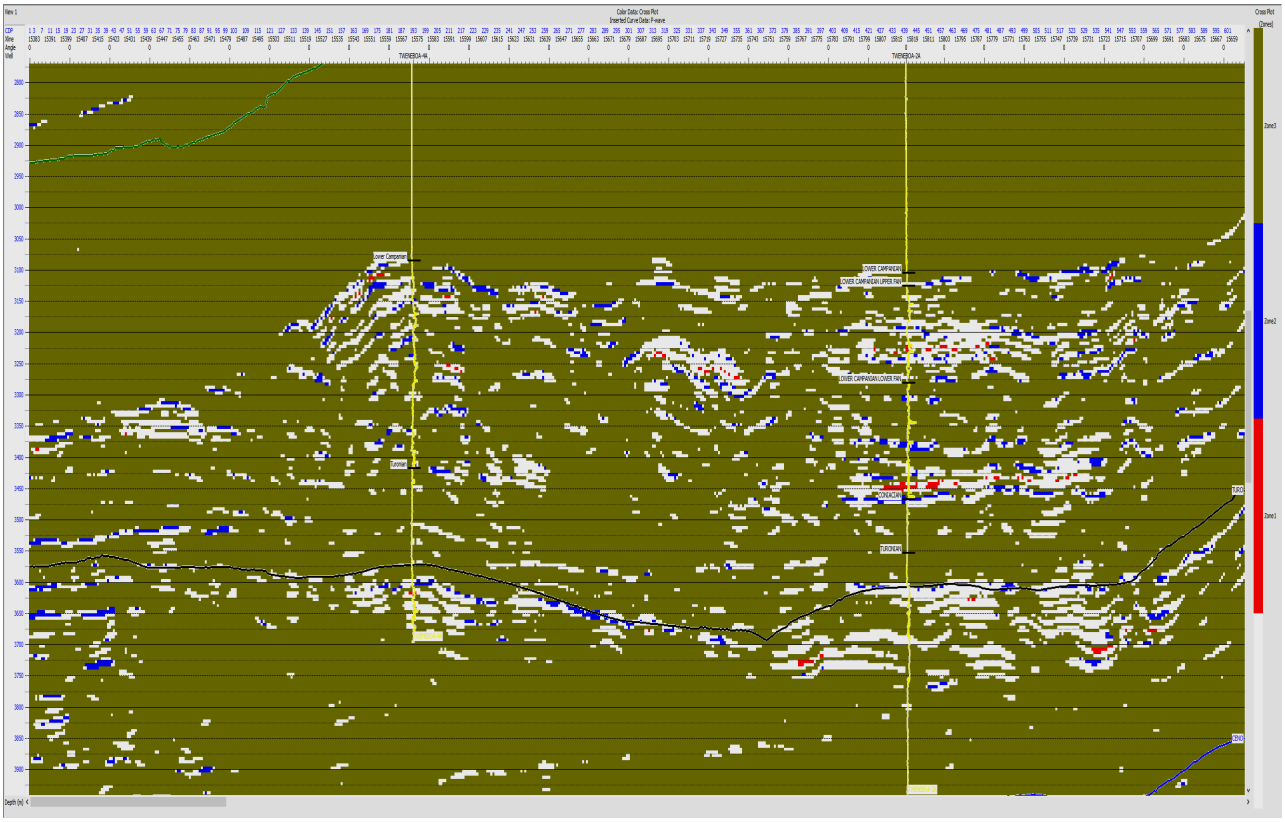

Figure 14. The three intercept-gradient clusters seen in section view for Case II.

shown by the yellow colour. A seismic reflection signal is produced by two factors: 1) an Acoustic term given by an acoustic impedance contrast and incident angle. 2) And a shear term given by a Poisson ratio contrast and incident angle/offset. The two may interfere constructively or destructively to amplify or attenuate the AVO response.

From **Figure 13**, the top of the gas sands is seen clustering in the region of Class II and III sands. The background and wet trends are seen in the green circle whiles the base of the gas sands is seen plotting in the blue region. The top of the gas sands is in the red region.

Areas in green constitute the background and wet trends. Potential top of hydrocarbon zones is in red whiles the base is in blue as shown in **Figure 14**.

5. Conclusion

The spectral balance process was performed to match the amplitude spectra of all angle stacks to that of the mid (26˚) stack on the test lines. The process had an effect primarily on the far (34˚ & 40˚) stacks. The frequency content of these stacks is slightly increased to match that of the near and mid stacks. The increase in frequency content of the events is observed on images of the far stacks from the test lines. In the offset scaling process, the RMS amplitude comparison between the synthetic and seismic suggests that the amplitude of the far traces should be reduced relative to the nearby up to 16%. However, the exact scaler

values depend on the time window considered. This suggests that the amplitude scaling with offset delivered from seismic processing is only approximately correct and needs to be checked with well synthetics and adjusted accordingly prior to use for AVO studies. The AVO attribute volumes generated were better at resolving anomalies on spectrally balanced and offset scaled data than data delivered from conventional processing.

Acknowledgements

The authors would like to thank the Ghana National Petroleum Corporation (GNPC) for the materials and resources. To Mr. Mohammed Abdul-Rahman (GNPC) for his supervision with the use of the Hampson Russel software.

Conflicts of Interest

The authors declare no conflicts of interest regarding the publication of this paper.

References

[1] Broadhead, R.F. (2002) The Origin of Oil and Gas in New Mexico's Energy, Present and Future: Policy, Production, Economics and the Environment. Brister, New Mexico.

[2] Petroleum System (2014) https://www.geologyin.com/2014/08/petroleum-system.html

[3] Young, R. and LoPiccolo, R. (2005) AVO Analysis Demystified. e-Seis.

[4] Shuey, R.T. (1985) A Simplification of the Zoeppritz Equations. *Geophysics*, **50**, 609-614. https://doi.org/10.1190/1.1441936

[5] Smith, G. and Gidlow, P. (1987) Weighted Stacking for Rock Property Estimation and Detection of Gas. *Geophysical Prospecting*, **35**, 993-1014. https://doi.org/10.1111/j.1365-2478.1987.tb00856.x

[6] Hilterman, F. (1975) Amplitudes of Seismic Seismic Waves: A Quick Look. *Geophysics*, **40**, 745-762. https://doi.org/10.1190/1.1440565

[7] Tetteh, J.T. (2016) The Cretaceous Play of Tano Basin, Ghana. *International Journal of Applied Science and Technology*.

[8] Binks, R.M. and Fairhead, J.D. (1992) A Plate Tectonic Setting for Mesozoic Rifts of West and Central Africa. *Tectonophysics*, **213**, 141-151. https://doi.org/10.1016/0040-1951(92)90255-5